

Characterization of an Open GTEM Cell with the COMSOL Multiphysics Software

A. De Vita¹, R. Gaffoglio² and B. Sacco^{1*}

¹ Centre for Research and Technological Innovation, RAI Radiotelevisione Italiana, Torino, Italy

² Istituto Superiore Mario Boella (ISMB), Torino, Italy

(The present work has been done when this author was with the Department of Physics of the University of Torino)

* Corresponding author: bruno.sacco@rai.it

Abstract: The Gigahertz Transverse Electromagnetic (GTEM) cell is a device used for generating known, homogeneous fields for calibration purposes and for studies on Electromagnetic Compatibility (EMC) on a wide frequency range. With the aid of the COMSOL Multiphysics[®] simulation software, we have analyzed the electromagnetic behavior of an existing open GTEM cell at different operating frequencies. This study allowed us to identify the region internal to the cell where the field is most purely TEM. Moreover, experimental values obtained using the real GTEM have been compared to the simulated results, providing a good agreement with them.

Keywords: COMSOL Multiphysics; GTEM cell; TEM mode; Voltage Standing Wave Ratio.

1. Introduction

The Gigahertz Transverse Electromagnetic (GTEM) cell is a fundamental tool for calibration purposes and for Electromagnetic Compatibility (EMC) studies, being able to simulate the effects of an incident plane wave (TEM mode) on the equipment under test in the GHz frequency band. This device is obtained by replacing one port of a two-port TEM cell with a wideband, resistor/wave absorber termination [1], which reduces the excitation of TE and TM modes at high frequencies. The resonances of the non-transverse field components can be further avoided by considering an open GTEM cell [2], derived from a conventional GTEM cell by physically removing the sidewalls. However, this open structure inevitably becomes more sensitive to the influence of the external environment, due to the absence of the screening by the lateral metal walls.

Since this tool is used for the calibration of precision instruments, it is of greatest importance to validate the uniformity of the field in the operating region. So, in the framework of a collaboration with RAI Way, we analyzed the electromagnetic behavior of the open GTEM cell whose geometrical dimensions are schematically reported in Fig. 1 and Table 1. In principle, the GTEM cell

can be considered as 50-ohm stripline, where the outer conductor is expanded pyramidally, while the central conductor (the GTEM septum) is a thin, wide conductive plate terminated by a combination of resistors and RF absorbers. Supposing to feed the GTEM cell with a 50 Ω coaxial cable, the geometrical design of the GTEM cell must ensure a matched characteristic impedance $Z_0 = 50 \Omega$ in all the sections along the longitudinal z direction [3,4]. The cell dimensions reported in Table 1, set by the manufacturer to guarantee a constant impedance along the cell, fit well the theoretical considerations reported in [5], where the singular-integral-equation technique has been used to derive the capacitance and hence the characteristic impedance of a rectangular coaxial line with a zero-thickness inner conductor.

A realistic reproduction of the Rai Way GTEM cell design has been implemented using the RF module of the COMSOL Multiphysics software. This paper reports the detailed description of the realized model (Section 2), focusing on the implementation of the backwall resistive termination, the RF absorbers, the feeding port and the boundary conditions imposed to correctly describe the system speeding up the computational time. Then, in Section 3, we report the simulated electric and

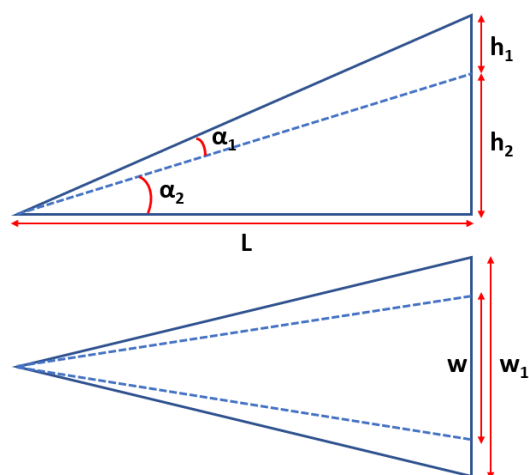


Figure 1. Geometry of the analyzed open GTEM cell; *upper row: lateral view, lower row: top view.*

Table 1. Geometrical dimensions of the GTEM cell. The first five parameters are expressed in cm.

L	h ₁	h ₂	w	w ₁	α ₁	α ₂
280	18.2	81.2	81.2	109.2	~3.2°	~16°

magnetic field patterns evaluated inside the cell, introducing a function suitable to estimate the purity of the propagating TEM mode. The simulations performed with COMSOL allowed us to compute the Voltage Standing Wave Ratio (VSWR) at the feeding port, whose value at different frequencies has been validated by the experimental results obtained performing a dense frequency sweep on the real GTEM cell (Section 4). Finally, the electric and magnetic field components evaluated with COMSOL in the GTEM internal test region have been compared to a series of field measurements performed using an electromagnetic scanner.

2. Open GTEM cell model

To analyze the electromagnetic behavior of the analyzed GTEM cell at different operating frequencies, we realized a realistic reproduction of the cell using the COMSOL Multiphysics software. Although the geometry and the dimensions of the cell faithfully reflect those of the real design, some simplifications have been introduced to keep the model compact and flexible as well as accurate, exploiting the potentialities of the software.

The geometry of the realized model is reported in Figures 2 and 3. As already emphasized, a GTEM cell can be intended as an extension of a 50-ohm transmission line expanding pyramidally, whose inner conductor is a thin metal layer called septum. Both the top and bottom surfaces, the back wall and the central septum have been modelled as infinitely thin two-dimensional layers with a Perfect Electric

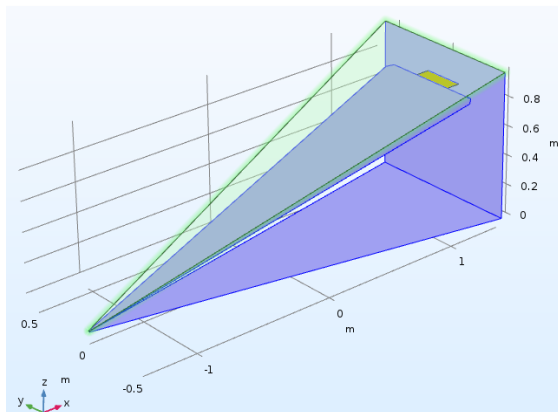


Figure 2. PEC condition on the GTEM cell geometrical structure; on the terminal part of the septum a transition boundary condition is introduced (yellow layer).

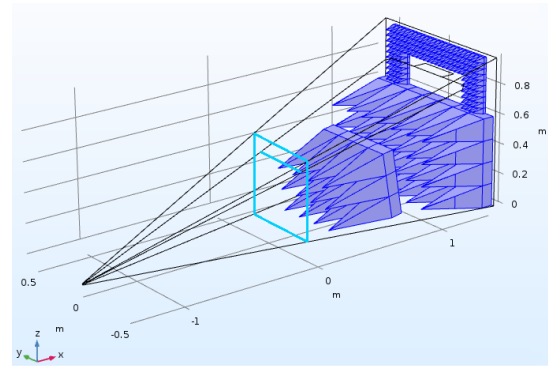


Figure 3. RF absorbers at the cell's backwall modelled with the COMSOL Multiphysics software.

Conductor (PEC) condition imposed on their surfaces. At the end of the existing cell, the current is terminated by a resistive network between the septum and the GTEM cell's backwall, practically realized by means of fifteen parallel series of five resistors having $R = 150 \Omega$; the overall resistance of the terminating network results:

$$R_{tot} = \left(\sum_{i=1}^{15} \frac{1}{R_s} \right)^{-1} = 50 \Omega, \quad (1)$$

where $R_s = 5 \cdot 150 \Omega = 750 \Omega$ is the resistance of each parallel series. Instead of modelling the resistive network, we decided to introduce a lossy layer between the septum and the backwall (see the yellow plane in Fig. 2), defined using a Transition Boundary Condition with a properly evaluated electric conductivity $\sigma = 0.71 \text{ S/m}$.

The electromagnetic fields in the real GTEM cell are terminated by three series of anechoic cones, reproduced in COMSOL as shown in Fig. 3. The geometry of each cell consists of one pyramid sitting on a block made of the same conductive material ($\sigma = 0.5 \text{ S/m}$) [6]. As illustrated in Fig. 4, at the interface of the conductive material and air, a process of partial reflection and partial transmission

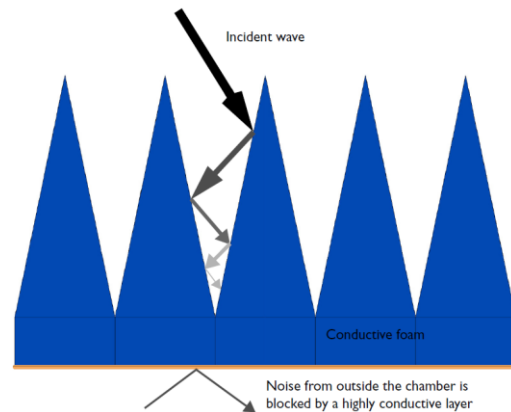


Figure 4. Process of partial reflection and partial transmission with subsequent attenuation through the anechoic cones [6].

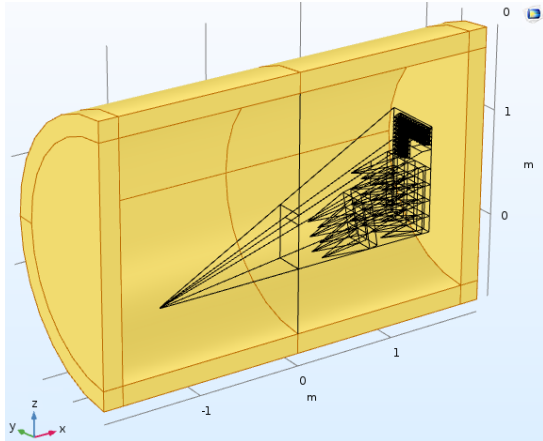


Figure 5. Introduction of a PMC symmetry plane to reduce the computational requirements.

with subsequent attenuation is repeated until the field reaches the base of the pyramid with a drastically reduced amplitude.

It should be noted that the bottom of the last series of absorbers coincides with the PEC backwall of the cell, useful to block any noise from the outside. The big RF absorbers have base side length $L = 15$ cm and total height $h \approx 52$ cm, while the dimensions of the small absorbers are: $L = 4$ cm, $h \approx 9$ cm. All the series of anechoic cones have been modelled using the COMSOL geometrical array function.

The feeding of the open GTEM cell has been modelled with a Multielement Lumped Port with characteristic impedance $Z_{ref} = 50 \Omega$ and fixed voltage V_0 , characterized by two Uniform Element sub-nodes, one defined between the septum and the upper side of the cell, and the other located between the septum and the cell lower plane, with an opposite field direction.

The GTEM cell has been inserted in a cylindrical air volume, wrapped by a cylindrical Perfectly Matched Layer (PML), created by means of an extrusion operation. Finally, a user-defined tetrahedral volume mesh has been defined, with a maximum element size fixed at $\lambda/5$, being λ the wavelength relative to the considered operating frequency.

Then, to reduce the computational demand, the model symmetry about the cell's longitudinal direction has been exploited by inserting a xz symmetry plane and removing half of the model domain, as shown in Fig. 5. Since on the $y = 0$ plane the z -directed electric field is symmetric, and the magnetic field is asymmetric, a Perfect Magnetic Conductor (PMC) condition was introduced [7]. This allows to obtain reliable simulation results with a lower computational demand. In this context, it should be noted that, since the symmetry plane also halves the lumped multielement feeding port, to preserve a correct

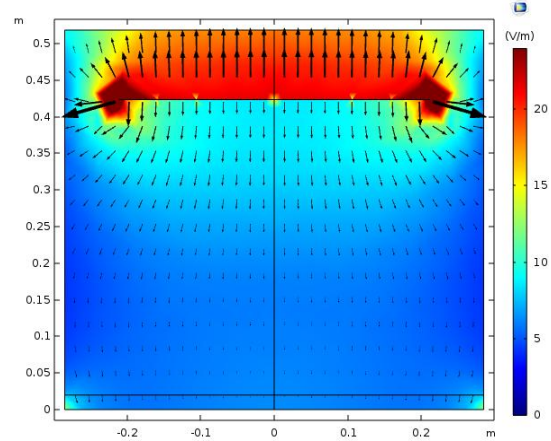


Figure 6. Electric field norm on the transversal plane highlighted in Fig. 3, at an operating frequency $f = 1$ GHz.

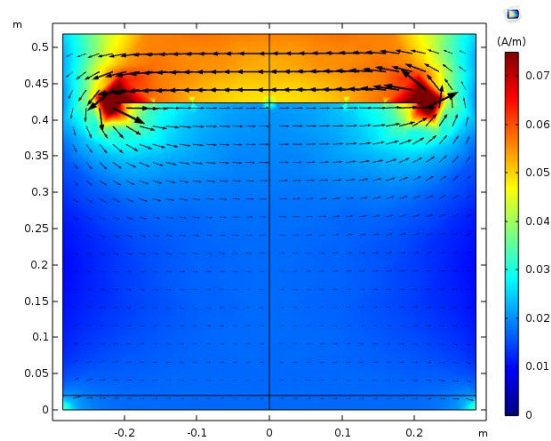


Figure 7. Magnetic field norm on the transversal plane highlighted in Fig. 3, at an operating frequency $f = 1$ GHz.

impedance matching along the cell it was necessary to double the port characteristic impedance, setting $Z_{ref} = 2 \cdot 50 \Omega$.

3. Simulation results

The designed COMSOL model has been computed for different values of frequencies: from 250 MHz to 1 GHz with steps of 50 MHz, and from 1 GHz to 3 GHz with steps of 200 MHz. At each frequency value, the TEM behavior in the cell was analyzed on the probing transversal yz plane highlighted in Fig. 3, where the electric and magnetic fields were computed. Fig. 6 and Fig. 7 show the electric and magnetic field, respectively, at the operating frequency $f = 1$ GHz; the portion of the field relative to the half of the GTEM cell excluded from the simulation domain has been obtained by symmetrizing the density plot.

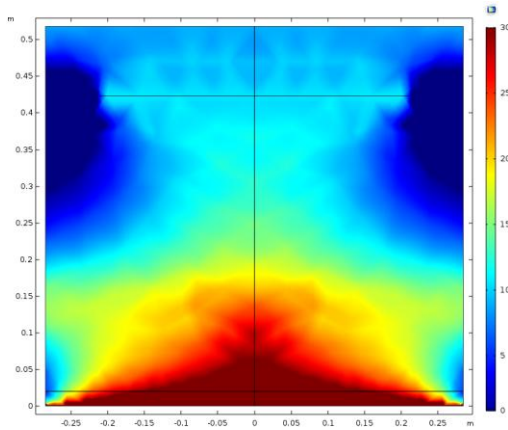


Figure 8. Axial ratio relative to the electric field, displayed on the transversal plane highlighted in Fig. 3, at $f = 1$ GHz.

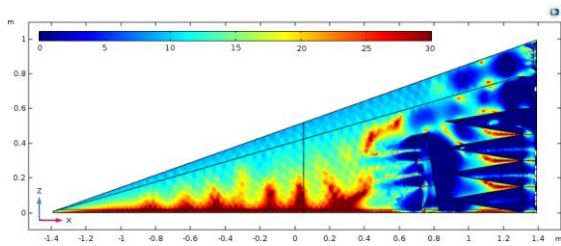


Figure 9. Axial ratio relative to the electric field, displayed on the cell longitudinal plane $y = 0$, at $f = 1$ GHz.

Furthermore, to estimate the purity of the propagating mode, we introduced the following function:

$$\text{Axial ratio (dB)} = 20 \log_{10} \left(\frac{|E_z|}{|E_{xy}|} \right) \quad (2)$$

where E_z is the transverse (vertical) component of the electric field. This expression, obtained using the fields computed by COMSOL, allowed us to identify the regions inside the cell where the propagating mode was most purely TEM (corresponding to those with a higher value of (2)). As expected, the strongest TEM behavior is observed near the cell lower plane; hence, in correspondence of the cell test volume (located around the transversal plane highlighted in Fig. 3), the EM waves basically propagate in transverse mode and therefore have the same characteristics as plane waves.

4. Experimental results

Rai Way provided us several experimental measurements performed with the real GTEM cell. Hence, to confirm the reliability of the COMSOL model, in this section we report a comparison between some of the most relevant experimental results and the corresponding simulated values.

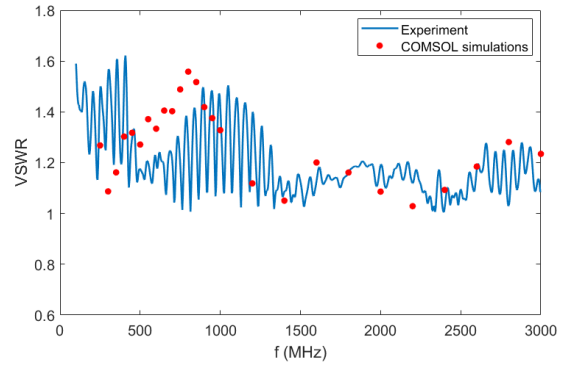


Figure 10. Voltage Standing Wave Ratio (VSWR) as a function of the operating frequency.

4.1 Voltage Standing Wave Ratio

The Voltage Standing Wave Ratio (VSWR) is a measure of the reflected power on a transmission line, representing power that is not accepted by the load and reflected back; it is defined by:

$$\text{VSWR} = \frac{1 + |S_{11}|}{1 - |S_{11}|} \geq 1 \quad (3)$$

where S_{11} is the reflection coefficient at the input port and $\text{VSWR} = 1$ implies a matched load [7].

COMSOL Multiphysics allowed us to directly compute the VSWR on the GTEM port at the different simulation frequencies; it was then possible to compare the simulated results to those obtained performing a dense frequency sweep on the real GTEM with a Vector Network Analyzer (VNA). The good agreement between the numerical and experimental results (see Fig. 10) validates the reliability of the implemented model at the considered different frequencies.

4.2 EM-Scan measurements



Figure 11. RFX EM-Scan inserted in the GTEM cell internal region.

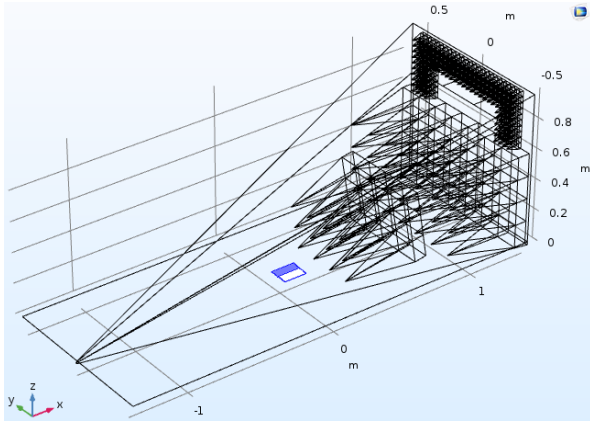


Figure 12. Region internal to the GTEM cell where the EM scanner was experimentally located.

The EM-Scan RFX is a compact bench-top electromagnetic (EM) scanner that allows a real-time antenna characterization in the laboratory environment with a broadband frequency coverage from 300 MHz to 6 GHz (see Fig. 11) [8]. The RFX scanner performs a very near field mapping of magnetic field and provides, by computation, the antenna's far-field patterns, bisections, EIRP (Effective Isotropic Radiated Power) and TRP (Total Radiated Power) with a scan time of a few seconds, as well as 2D and 3D near-field patterns, including amplitude, phase and polarization.

To evaluate the field components inside the GTEM cell, the EM scanner (Fig. 11) has been inserted in the GTEM cell test volume, in correspondence of the region highlighted in Fig. 12. The surface of the considered RFX scanner is characterized by $24 \times 16 = 384$ H-field probes, distributed over a rectangular region with dimensions 16 cm \times 10 cm. Since the electromagnetic field uniformity in the test region of a GTEM cell is a basic prerequisite for making the measurements reproducible [9], we report in Fig. 13 the expression:

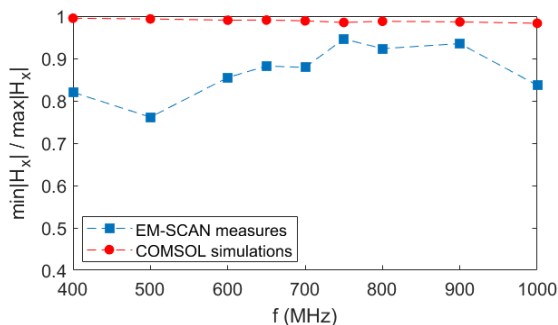


Figure 13. Expression (4) evaluated at different frequencies using both the EM-scanner measures and the COMSOL simulation results.

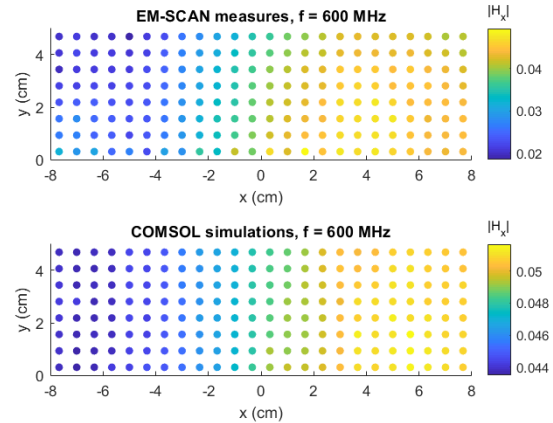


Figure 14. Amplitude of the magnetic field x -component directly estimated with the RFX scanner (upper row) and simulated with COMSOL Multiphysics (lower row), at $f = 600$ MHz, on the test region highlighted in Fig. 12.

$$\frac{\min |H_x|}{\max |H_x|} \leq 1 \quad (4)$$

where H_x is the magnetic field component along the x -axis, relative to the propagating TEM mode, while the \min and the \max functions have been calculated over the region highlighted in Fig. 12. Fig. 13 shows (4) as a function of frequency, evaluated using the experimental magnetic field measurements obtained with the RFX scanner as well as the simulations performed with COMSOL. As can be observed, a uniform field distribution can be attained in the test core of the cell and a sufficiently good agreement between simulated and measured H-field values occurs.

In Fig. 14 it is also reported a direct comparison between the amplitudes of the magnetic field x -component ($|H_x|$) evaluated with the EM scanner and those simulated with COMSOL Multiphysics, at $f = 600$ MHz. The data set corresponds to the 24×8 H-field probe grid of the EM scanner included in the half of the model directly simulated with COMSOL, i.e., not symmetrized (see the blue highlighted region in Fig. 12). A good agreement between the measured and simulated results is observed.

5. Conclusions

In this paper we have presented the implementation of a flexible, reproducible and reliable model of an existing GTEM cell, realized with the COMSOL Multiphysics software.

The regions inside the cell where the electromagnetic field was most purely TEM have been detected, introducing some significant expressions of the fields components, evaluated with the COMSOL software in post-processing.

A strong TEM behavior and a good uniformity, expressed in terms of H-field minimum to maximum ratio, has been demonstrated in the region corresponding to the test volume of the real GTEM cell. Moreover, we have shown how the COMSOL Multiphysics proved to be a very efficient tool for our analyses, allowing us to get reliable results in good agreement with a large series of experimental measures.

6. References

- [1] D. Königstein and D. Hansen, "A New Family of TEM-cells with Enlarged Bandwidth and Optimized Working Volume", *Proceedings of the 7th International Zurich Symposium on Electromagnetic Compatibility*, 127-130, Zurich (1987).
- [2] R. Rambousky and H. Garbe, "Analysis of Open TEM-Waveguide Structures", *Ultra-Wideband, Short-Pulse Electromagnetics 10*, 49-58, Springer, New York (2014).
- [3] M. Bozzetti, et al., "Characterization of a GTEM cell designed for the SAR evaluation in in vitro experiments", *PIER Symposium 2004*, Pisa.
- [4] W.-T. Shay, W.-P. Hong, R.-R. Lao and J.-H. Tarng, "Design Methodology and Performance Evaluation of a Tapered Cell", *IEEE Trans. Instrum. Meas.*, vol. 62, no. 6, pp. 1821-27, 2013.
- [5] J. C. Tippet and D. C. Chang, "Characteristic Impedance of a Rectangular Coaxial Line with Offset Inner Conductor", *IEEE Trans. Microw. Theory Tech.*, vol. 26, no. 11, pp. 876-883, 1978.
- [6] *Modeling of Pyramidal Absorbers for an Anechoic Chamber*, COMSOL Multiphysics.
- [7] D. M. Pozar, *Microwave Engineering*, 4th ed. John Wiley and Sons, Inc., 2011.
- [8] *EM-Scan-RFX2-Datasheet*, Calgary, Canada.
- [9] G. Calò, F. Lattarulo and V. Petruzzelli, "GTEM Cell Experimental Set up for In Vitro Dosimetry", *Journal of Communications Software and Systems*, vol. 3, no. 1, pp. 34-43, 2007.

7. Acknowledgments

We would like to thank the whole COMSOL technical support staff in Brescia for their availability and help, with particular regard to Gabriele Rosati, and Eng. Aldo Scotti, from RAI and Eng. Giuseppina Moretti, from Rai Way, for providing us all the experimental measurements.